Available online at www.sciencedirect.com

SCIENCE DIRECT

Cement and Concrete Research 35 (2005) 1233–1246

Cement and Concrete Research

Durability of geopolymer materials in sodium and magnesium sulfate solutions

T. Bakharev

Department of Civil Engineering, Monash University, Clayton, Victoria 3800, Australia

Received 11 November 2003; accepted 9 September 2004

Abstract

This paper presents an investigation into the durability of geopolymer materials manufactured using class F fly ash and alkaline activators when exposed to a sulfate environment. Three tests were used to determine resistance of geopolymer materials. The tests involved immersions for a period of 5 months into 5% solutions of sodium sulfate and magnesium sulfate, and a solution of 5% sodium sulfate+5% magnesium sulfate. The evolution of weight, compressive strength, products of degradation and microstructural changes were studied.

In the sodium sulfate solution, significant fluctuations of strength occurred with strength reduction 18% in the 8FASS material prepared with sodium silicate and 65% in the 8FAK material prepared with a mixture of sodium hydroxide and potassium hydroxide as activators, while 4% strength increase was measured in the 8FA specimens activated by sodium hydroxide. In the magnesium sulfate solution, 12% and 35% strength increase was measured in the 8FA and 8FAK specimens, respectively; and 24% strength decline was measured in the 8FASS samples. The most significant deterioration was observed in the sodium sulfate solution and it appeared to be connected to migration of alkalies into solution. In the magnesium sulfate solution, migration of alkalies into the solution and diffusion of magnesium and calcium to the subsurface areas was observed in the specimens prepared using sodium silicate and a mixture of sodium and potassium hydroxides as activators. The least strength changes were found in the solution of 5% sodium sulfate+5% magnesium sulfate. The material prepared using sodium hydroxide had the best performance, which was attributed to its stable cross-linked aluminosilicate polymer structure.

Keywords: Durability; Sulfate attack; Fly ash; Alkali-activated cement; Microstructure

1. Introduction

Sulfate attack is an important durability and serviceability concern for geopolymer materials used in construction. Previous experience with Portland cement and blended cement concretes showed cases of concrete deterioration when exposed to sulfate attack in the environment [1–3]. Studies of the sulfate attack on OPC concrete revealed that it has a complicated mechanism, and due to reactions between cement hydration products and sulfate-bearing solutions, it manifests itself in a variety of ways. Studies of the external sulfate attack on OPC concrete show that reactions involve CH, C–S–H and the aluminate component of hardened cement paste [4,5]. As a result of these reactions, expansion and cracking are caused, directly or indirectly, by ettringite and gypsum formation, while softening and disintegration are caused by destruction of C–S–H [4–6]. In case of magnesium sulphate attack, layers of brucite and gypsum were formed in the surface area, while in transition zone adjacent to the surface, C–S–H became depleted in Ca [7,8].

Geopolymer concrete is a novel material prepared using alkali-activated fly ash as the only binder. Environmental and economic benefits of using geopolymer materials are due to utilisation of wastes from energy manufacture, 80% of which are not utilised and have to be land filled. Previous publications on geopolymer materials investigated the effect of curing procedures, water/binder ratio and composition of the alkaline solution on strength develop-

E-mail address: tbakharev@optusnet.com.au.

0008-8846/$ - see front matter © 2004 Elsevier Ltd. All rights reserved.
doi:10.1016/j.cemconres.2004.09.002

Table 1
Composition of fly ash (mass%) by XRF

Oxide	SiO_2	Al_2O_3	Fe_2O_3	CaO	MgO	K_2O	Na_2O	TiO_2	P_2O_5	Loss on ignition
Fly ash	50.0	28.0	12.0	6.5	1.3	0.7	0.2	–	–	–

ment and hydration products [9–13]. The geopolymer materials are prepared using w/b=0.2–0.4, and w/b=0.3 is most commonly used. The alkaline solution usually contains sodium silicate, sodium and sometimes potassium hydroxides. The geopolymerisation reaction is performed under basic conditions in the presence of alkali metal salts or hydroxides, which are necessary for dissolution of the starting materials and also for the catalysis of condensation reactions [14,15]. Hydrothermal curing greatly accelerates these reactions, and hence, strength development in geopolymer materials. Geopolymer concretes possess hardness 70–110 VHN and have strength 40–70 MPa [9,11–13]. Previous papers presented processing and characterisation of the geopolymer materials and a study of durability in case of acid attack [11,16]. Durability of geopolymer materials in sulfate environment was not investigated before; however, there is an opinion that geopolymers have excellent resistance in sulfate environment due to absence of high-calcium phases. Chemical composition of geopolymer materials include ~50% SiO_2, ~30% Al_2O_3, 8–9% Na_2O, 2–8% CaO, which differs from OPC (~20% SiO_2, ~1–5% Al_2O_3, ~65% CaO). The geopolymer materials in this investigation contained 6.5% CaO and had phase composition significantly different from OPC. This paper presents an investigation of sulfate attack on geopolymeric materials prepared using class F fly ash and sodium silicate, potassium hydroxide and sodium hydroxide activators and cured hydrothermally at 95 °C.

2. Experimental

2.1. Materials

The chemical and mineral compositions of fly ash are shown in Table 1 and Fig. 1, respectively. Fly ash used was sourced from Gladstone in Queensland, Australia. It is mainly glassy with some crystalline inclusions of mullite, hematite and quartz. Laboratory-grade sodium silicate solution type D with Ms (ratio of silica oxide to sodium oxide) equal to 2, 14.7% Na_2O and 29.4% SiO_2 was supplied by PQ Australia, while 60 w/v% sodium hydroxide solution was supplied by Sigma. Ninety-eight percent analytical-grade potassium hydroxide was supplied by Sigma. Sodium hydroxide, potassium hydroxide and sodium silicate solutions were used for fly ash activation.

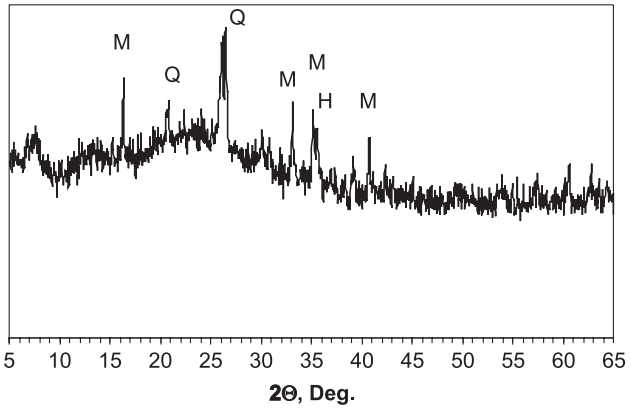

Fig. 1. XRD traces of fly ash. Q=quartz, M=mullite, H=hematite.

2.2. Test procedures

Fly ash was activated by sodium hydroxide, a mixture of sodium and potassium hydroxides and sodium silicate solutions, providing 8–9% Na in mixtures and water/binder ratio of 0.3; Table 2 shows the details of the samples and curing conditions. The pastes were cast in plastic cylinders and sealed with the lid. The mixtures were cured for 24 h at room temperature; after that, the mixtures were ramped to 95 °C and cured at this temperature for 24 h, and then the materials cooled down with the oven and were cured at room temperature for 2 days prior to test. The initial strength of samples prior to tests was: 58 MPa 8FAK, 66 MPa 8FASS and 59.5 MPa 8FA.

The resistance of materials to sulfate attack was studied by immersion of specimens in 5% solutions of sodium and magnesium sulfate, and solution of 5% sodium sulfate+5% magnesium sulfate. ø25×50 mm cylinders were immersed into 30-l drums with testing solutions. The compressive strength of ø25×50 mm cylinders was measured before the test and at 30, 60, 90, 120 and 150 days. Neat Portland cement paste (OPC) and Portland cement paste with 20% fly ash replacement (OPC+FA) with water/binder ratio 0.4 were used for comparison in the tests as having the same consistency as geopolymeric specimens at the time of

Table 2
Geopolymer samples

Sample ID	Type of activator and w/b ratio	Concentration	Curing conditions
8FASS	Sodium silicate, w/b=0.3	8% Na	24 h at room temp., 24 h at 95 °C for all cases
8FA	Sodium hydroxide, w/b=0.3	8% Na	
8FAK	Sodium hydroxide+ Potassium hydroxide, w/b=0.3	8% Na +1%K	

Table 3
Weight changes of the samples exposed to 5% solutions of sodium and magnesium sulfate, and solution of 5% sodium sulfate+5% magnesium sulfate

Sample ID	5% Na_2SO_4	5% $MgSO_4$	5% Na_2SO_4+ 5% $MgSO_4$
8FA	3.1%	1.4%	2.1%
8FASS	4.7%	5.3%	0.4%
8FAK	1.3%	−1.02%	1.5%
OPC	3.2%	6.16%	9.1%
OPC+FA	2.35%	3.17%	7.3%

molding. The compressive strength of these specimens at the age of 2 months when the test started was 45 and 42.9 MPa, respectively.

The deterioration was studied by X-ray diffraction (XRD), Fourier transform infrared spectroscopy (FTIR) and scanning electron microscopy (SEM). For the analysis, the samples were taken from the surface (0–1 mm depth) exposed to the solutions. X-ray diffraction analyses were made with a Rigaku Geigerflex D-max II automated diffractometer with the following conditions: 40 kV, 22.5 mA, Cu-Kα radiation. The XRD patterns were obtained by scanning at 0.1° (2θ) per min and in steps of 0.05° (2θ). Fourier transform infrared spectroscopy (FTIR) was performed for the samples on Perkin Elmer 1600 spectrometer using the KBr pellet technique (3 mg powder sample mixed with 100 mg KBr).

Microstructural studies utilised SEM (Hitachi S-2300, Japan) equipped with EDS analyser (Oxford Image Analysis). Secondary electron images were collected of the fractured specimens, and polished specimens were studied in backscattered electrons. To prepare polished specimens, 1-mm-thick slices were cut using a low-speed diamond saw. The samples were first impregnated with ultralow viscosity resin and then polished. All the specimens were carbon coated. X-ray microanalyses were carried out at an accelerating voltage of 20 kV for 200 s; matrix corrections applied by ZAF procedure.

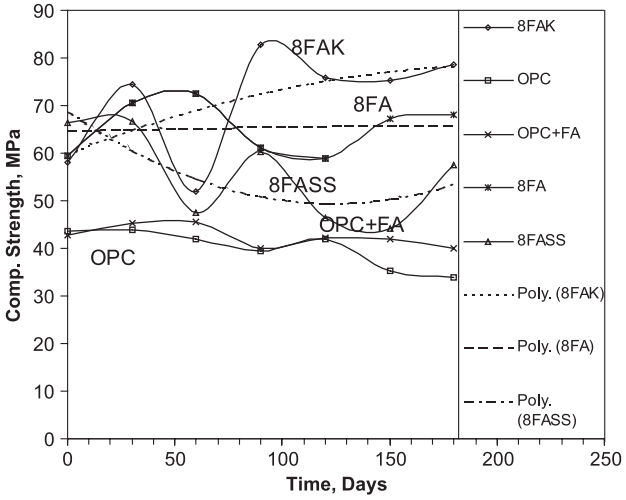

Fig. 3. Compressive strength evolution of the geopolymer and Portland cement specimens exposed to 5% magnesium sulfate solution.

3. Results

Geopolymer samples exposed to sulfate solutions had no visual signs of deterioration. After months of exposure to sulfate solutions, the surface of the samples had no deposits and was as smooth as immediately before the test. However, there were some weight changes in the samples after 5 months of immersion (Table 3). The 8FA samples prepared using sodium hydroxide activator gained 3.1% in the sodium sulfate, and 1.4% in the magnesium sulfate solutions. The 8FASS samples prepared using sodium silicate activator gained 4.7% in the sodium sulfate and 5.3% in the magnesium sulfate solutions. The 8FAK samples prepared using a mixture of sodium and potassium

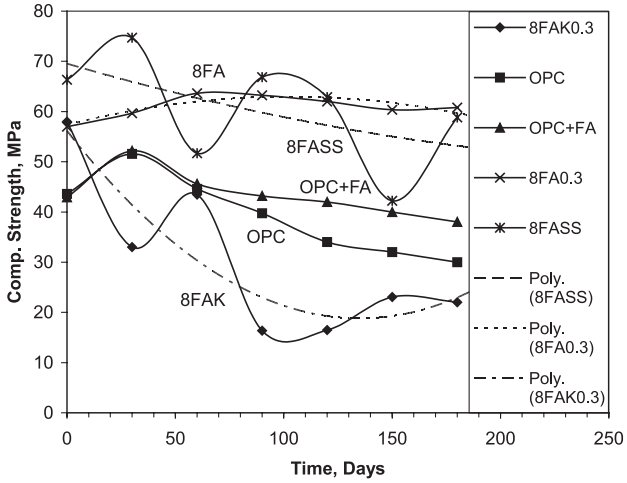

Fig. 2. Compressive strength evolution of the geopolymer and Portland cement specimens exposed to 5% sodium sulfate solution.

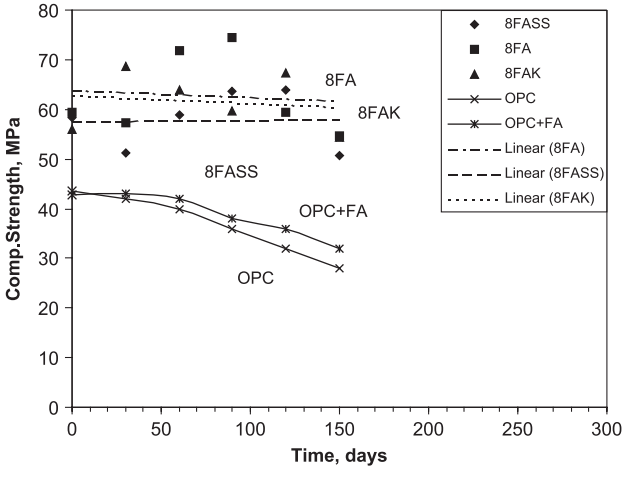

Fig. 4. Compressive strength evolution of the geopolymer and Portland cement specimens exposed to a solution of 5% sodium sulfate+5% magnesium sulfate.

Table 4
Summary of compressive strength evolution in sulphate environment (%)

Sample ID	Na_2SO_4 solution (%)	$MgSO_4$ solution (%)	Na_2SO_4+$MgSO_4$ solution (%)
8FA	+4	+12	+12
8FAK	−65	+35	+10
8FASS	−18	−24	−4.5
OPC	−30	−21	−35
OPC+FA	−14	−4.8	−19

hydroxides gained 1.3% in the sodium sulfate and lost 1.02% in the magnesium sulfate solutions. In the solution of sodium sulfate+magnesium sulfate, the geopolymer samples had the least weight changes: 2.1% weight gain in the 8FA, 0.4% in the 8FASS and 1.5% in the 8FAK samples.

OPC and OPC+FA samples had some changes in appearance: in the solution of magnesium sulfate, the samples became covered by 1-mm-thick white cover, while in the solution of sodium sulfate, there was cracking along the corners of the specimens. OPC+FA samples had less deterioration than OPC samples, which had the most significant changes in weight and strength after tests. In the solution of sodium+magnesium sulfate, OPC and OPC+FA samples experienced the most significant deterioration and gained weight, 9.1% and 7.3%, respectively.

3.1. Compressive strength

Figs. 2–4 show compressive strength evolution of the specimens in different sulphate solutions. In Figs. 2–4, dotted lines present the polynomial trendlines of strength evolution. Table 4 gives a summary of strength evolution in different sulphate environments. In the sodium sulfate solution, the 8FA samples prepared using sodium hydroxide performed better than the 8FAK and 8FASS samples and had 4% strength increase over the time of experiment. In the same environment, compressive strength of the 8FASS and

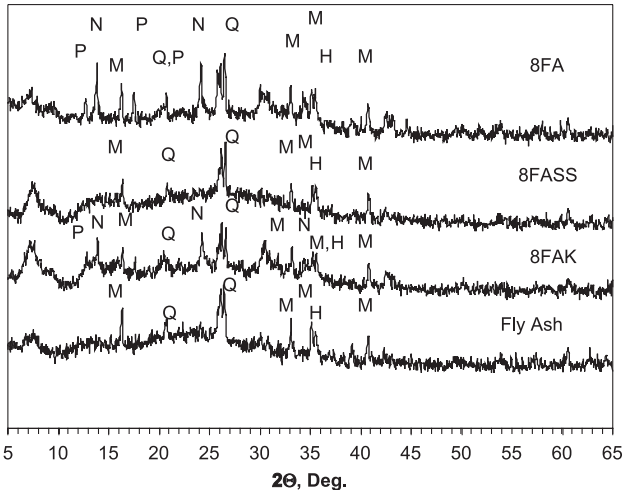

Fig. 5. XRD analysis of the geopolymer materials before tests: (a) 8FA, (b) 8FASS, (c) 8FAK. P=Na-P1 (gismondine), N=hydroxysodalite, Q=quartz, M=mullite, H=hematite.

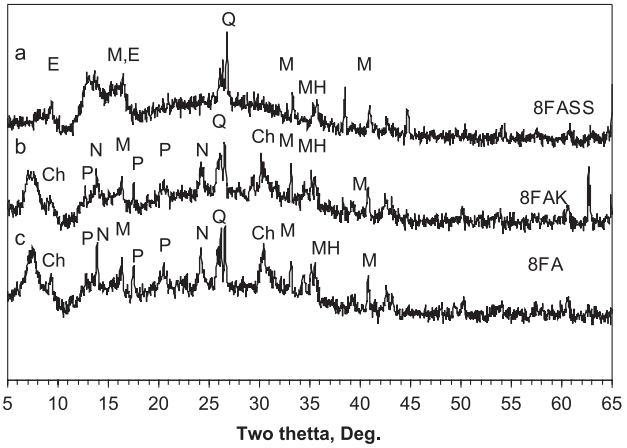

Fig. 6. XRD traces of the geopolymer materials after 2 months exposure to 5% sodium sulfate solution: (a) 8FASS, (b) 8FAK, (c) 8FA: Ch=chabazite, P=Na-P1 (gismondine), N=hydro-sodalite, E=ettringite, Q=quartz, M=mullite, H=hematite.

8FAK samples fluctuated and significantly declined from the initial value, with 18% reduction in the 8FASS specimens and 65% reduction in the 8FAK specimens. Some fluctuation of strength was observed in all geopolymer specimens in the magnesium sulfate solution. Compressive strength of the specimens finally equilibrated with 35% and 12% strength increase compared to the initial value in the 8FAK and 8FA specimens, respectively. However, in this solution, 24% strength decline was measured in the 8FASS samples. The best overall performance of the geopolymer samples was in the solution of sodium sulfate+magnesium sulfate, where 12% and 10% strength increase was found in the 8FA and 8FAK specimens, respectively, and 4.5% strength reduction in the 8FASS specimens. In sulfate solutions, strength of OPC and FA+OPC specimens increased in the first month of the test, and then had a steady decline. After 5 months of the test, the loss of strength was up to 35% for OPC and 19% for OPC+FA specimens.

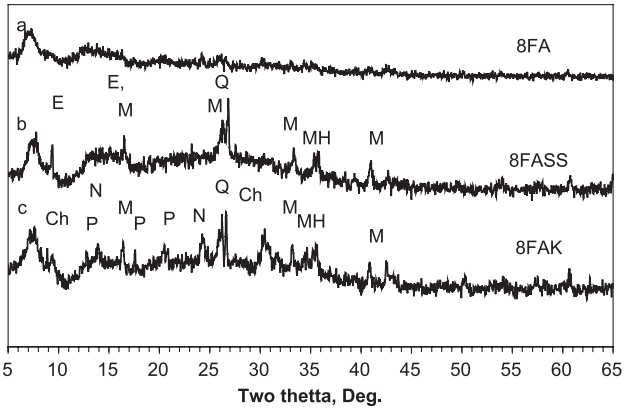

Fig. 7. XRD traces of the geopolymer materials after 2 months exposure to 5% magnesium sulfate solution: (a) 8FA, (b) 8FASS, (c) 8FAK: Ch=chabazite, P=Na-P1 (gismondine), N=hydro-sodalite, E=ettringite, Q=quartz, M=mullite, H=hematite.

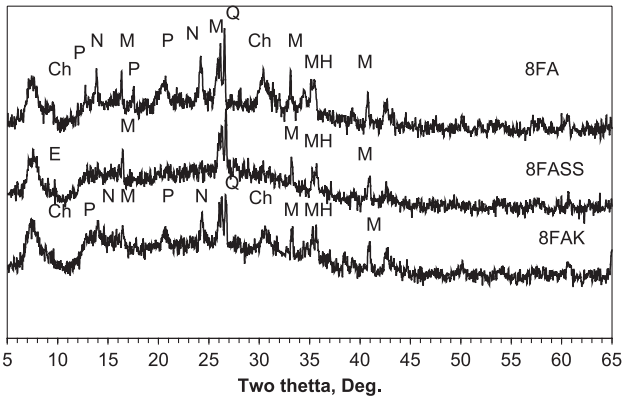

Fig. 8. XRD traces of the geopolymer materials after 3 months exposure to solution of 5% sodium sulfate+5% magnesium sulfate: (a) 8FA, (b) 8FASS, (c) 8FAK. Ch=chabazite, E=ettringite, P=Na-P1 (gismondine), N=hydro-sodalite, Q=quartz, M=mullite, H=hematite.

3.2. X-ray diffraction

Fig. 5 shows XRD traces of the geopolymer samples before the test. Peaks due to quartz, mullite and hematite of the crystalline component of the fly ash can be seen in addition to a broad peak in the region 17–35° 2θ arising from the glassy phase of the fly ash and broad peaks in the regions 6–10° and 12–16° 2θ arising from aluminosilicate gel. In addition, peaks for hydro-sodalite and Na-P1 (gismondine) zeolites were present in the XRD spectra of the 8FA and 8FAK specimens. The 8FA specimen contained more ordered hydro-sodalite and Na-P1 (gismondine) zeolite than the 8FAK specimen.

For the analysis, the samples were taken from the surface (0–1 mm depth) exposed to solutions. Fig. 6 presents XRD traces of the geopolymer materials exposed to 5% sodium sulfate solution for 2 months. A broad peak in the region 12–17° 2θ arising from aluminosilicate gel appeared in the XRD spectrum of the 8FASS specimen. Traces of chabazite can be seen in the spectra of the 8FA and 8FAK specimens, and traces of ettringite in the spectrum of the 8FASS specimen can be seen after the exposure. The most significant changes were observed in the spectrum of the 8FASS specimen, while the XRD spectra of the 8FA and 8FAK specimens had the least changes.

Fig. 7 presents XRD traces of the geopolymer materials exposed to 5% magnesium sulfate solution for 2 months. In the 8FA XRD spectrum, traces of fly ash, hydroxysodalite and Na-P1 were not seen and a broad peak at 7–9° 2θ arising from aluminosilicate gel was observed instead. It is proposed that disappearance of peaks of quartz and some other crystalline residue of fly ash is due to these crystals being covered by amorphous phases formed as a result of reaction of aluminosilicate gel with magnesium sulfate solution, so that they become invisible in XRD pattern. Traces of chabazite and ettringite appeared in a spectrum of the 8FAK specimen. In the 8FASS specimen, new phase appeared which was identified based on XRD and SEM data as the ettringite phase.

Fig. 8 presents XRD traces of the geopolymer materials after 3 months exposure to the 5% sodium sulfate+5%

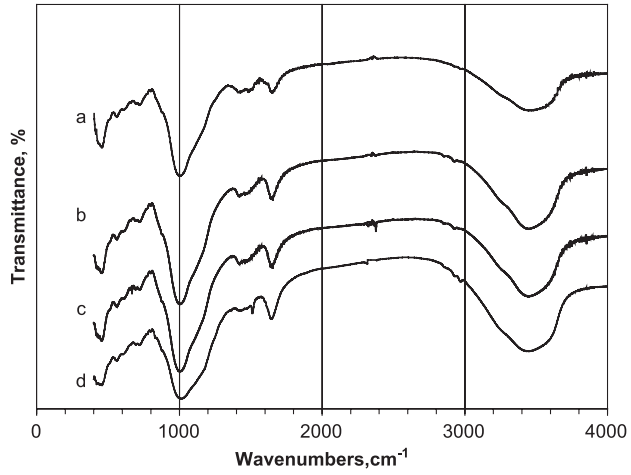

Fig. 10. FTIR of geopolymer samples 8FAK (a) before tests, and after 1 month exposure to (b) 5% Na_2SO_4 solution, (c) 5% $MgSO_4$ solution and (d) 5% Na_2SO_4+5% $MgSO_4$ solution.

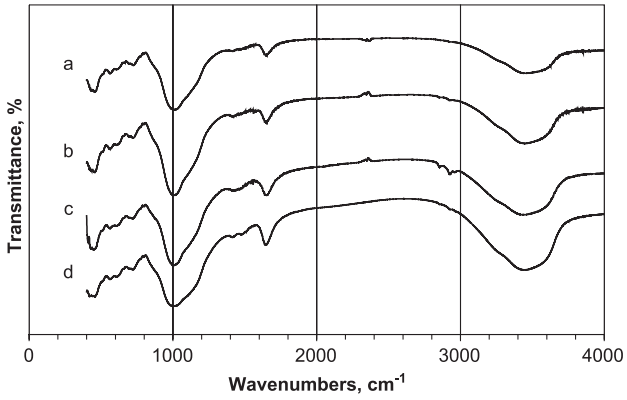

Fig. 9. FTIR of geopolymer samples 8FA prepared using sodium hydroxide (a) before tests, and after 1 month exposure to (b) 5% Na_2SO_4 solution, (c) 5% $MgSO_4$ solution and (d) 5% Na_2SO_4+5% $MgSO_4$ solution.

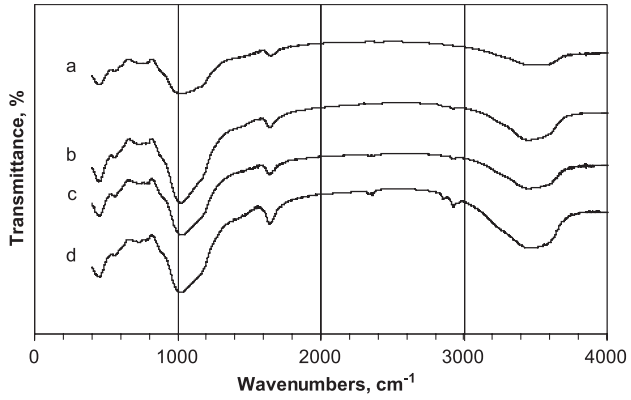

Fig. 11. FTIR of geopolymer samples 8FASS (a) before tests, and after 1 month exposure to (b) 5% Na_2SO_4 solution, (c) 5% $MgSO_4$ solution and (d) 5% Na_2SO_4+5% $MgSO_4$ solution.

Table 5
Characteristic IR vibrational bands of the geopolymer materials

Wavenumber (cm^{-1})	Assignment
3700–3600 (s)	Stretching vibration (–OH)
3600–2200 (s)	Stretching vibration (–OH, HOH)
1700–1600	Bending vibration (HOH)
1200–950 (s)	Asymmetric stretching (Si–O–Si and Al–O–Si)
1100 (sh)	Asymmetric stretching (Si–O–Si)
850 (sh)	Si–O stretching, OH bending (Si–OH)
795(m)	Symmetric stretching (Si–O–Si)
688 (sh)	Symmetric stretching (Si–O–Si and Al–O–Si)
520–532(m)	Double ring vibration
424 (s)	Bending (Si–O–Si and O–Si–O)

s, strong; w, weak; m, medium and sh, shoulder.

magnesium sulfate solution. When compared to the XRD spectra of the specimens before the exposure (Fig. 5), it can be seen that the least changes took place in this solution. Traces of chabazite appeared in the spectra of the 8FA and 8FAK specimens, and traces of ettringite were found in the spectrum of the 8FASS specimen. Traces of hydro-sodalite and Na-P1 persisted in the 8FA and 8FAK specimens. In addition, broad peaks at 7–9° and at 12–16° 2θ arising from aluminosilicate gel were also present in the XRD spectra of the 8FAK and 8FA specimens.

3.3. Infrared spectroscopy (FTIR)

Figs. 9–11 present IR spectra of the geopolymer materials before the test and after exposure to different sulfate solutions. For the analysis, the samples were taken from the surface (0–1 mm depth) exposed to solutions. The attribution of the IR spectral bands was performed using zeolite IR assignments given in Ref. [15]. Table 5 shows the assignment of the characteristic IR vibrational bands. The strongest vibration at 970–1000 cm^{-1} is assigned to asymmetrical Si–O stretch. The next strongest band at 424 cm^{-1} is assigned to a Si–O bending mode. The Si–O–Si symmetrical stretching vibrations are assigned in 688 cm^{-1} region. The Si–OH stretching modes are assigned in the region 850 cm^{-1}. Vibrations assigned to double ring are in 520–532 cm^{-1} region. The stretching modes are sensitive to the Si–Al composition of the framework and may shift to a lower frequency with increasing number of tetrahedral aluminium atoms [15]. Thus, asymmetric stretch Al–O–Si was assigned in 974 cm^{-1}, while Si–O–Si stretch was assigned in 1084 cm^{-1} region. The vibrations assigned to bending (H–O–H) and stretching of (OH)–groups were observed in 1600 and 3450 cm^{-1} regions, respectively.

Fig. 9 presents FTIR spectra of the 8FA specimens prepared using sodium hydroxide. In the result of exposure to sodium sulfate, magnesium sulfate and magnesium

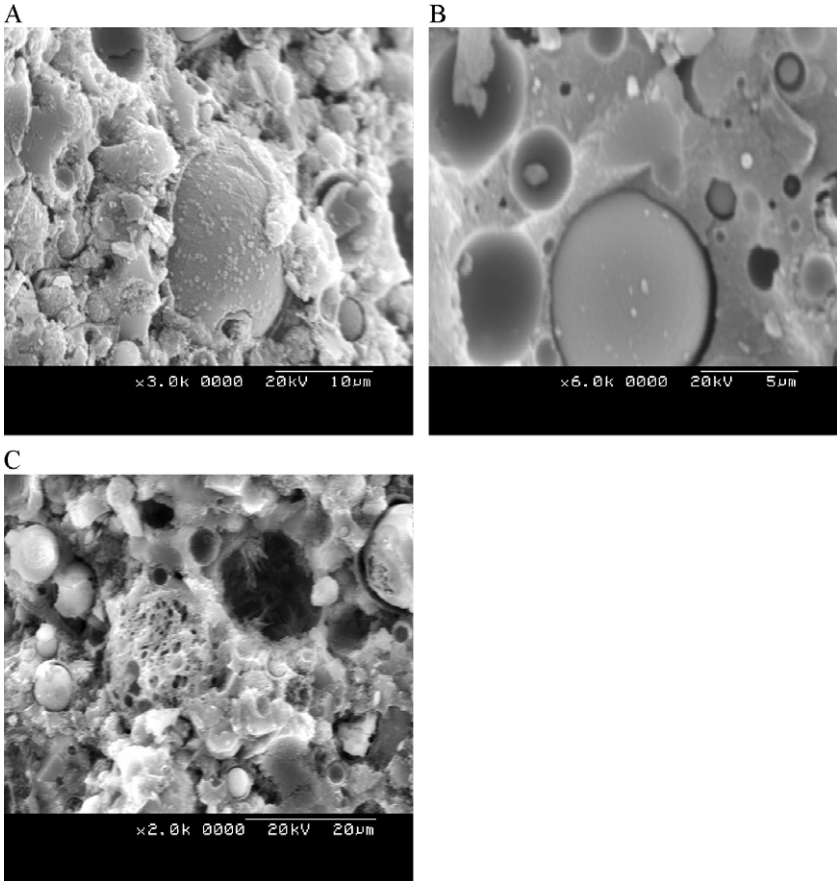

Fig. 12. SEI of geopolymer samples before the test: (A) 8FA, (B) 8FASS, (C) 8FAK.

sulfate+sodium sulfate solutions, the asymmetrical Si–O–Al and Si–O–Si stretching vibrations at 974 and 1084 cm^{-1}, respectively, had no shift, but the bands became of higher intensity. There were no significant changes in all other bands, insignificant shifts occurred in the double ring vibrations band located in 524–594 cm^{-1} region in the magnesium sulfate solution.

Fig. 10 presents FTIR spectra of the 8FAK specimens prepared using a mixture of sodium and potassium hydroxide solutions. There were no significant shifts of the spectral bands in all solutions. In the sodium and magnesium sulfate solutions, the asymmetrical Si–O–Al and Si–O–Si stretching vibrations at 974 and 1084 cm^{-1}, respectively, have increased their intensity. In the magnesium sulfate+sodium sulfate solution, a significant increase of intensity of the asymmetrical Si–O–Si stretching vibrations at 1084 cm^{-1} was observed.

Fig. 11 presents FTIR spectra of the FASS specimens prepared using sodium silicate before the test and after immersion into different sulfate solutions. In the result of exposure to sodium sulfate, magnesium sulfate and magnesium sulfate+sodium sulfate solutions, the asymmetrical Si–O–Al and Si–O–Si stretching vibrations at 974 and 1084 cm^{-1} shifted to higher frequency 992 and 1128 cm^{-1}, respectively, and became of higher intensity, while the Si–O–Si and Si–O–Al symmetric stretching vibrations in 688 cm^{-1} region shifted to 688–742 cm^{-1}. There was a significant increase in intensity of the asymmetric Si–O–Si stretching vibrations at 1128 cm^{-1} after exposure to the magnesium sulfate+sodium sulfate solution.

To summarise, after exposure to 5% sodium sulfate and 5% magnesium sulfate solutions, in the 8FA, 8FASS and 8FAK specimens, there was an increase of a mean chain length of aluminosilicate polymers, which was evident from the increase of intensity of the spectral bands. In addition, there was an increase of Si/Al atom ratio in the polymers of the 8FASS specimen. After exposure to the 5% sodium sulfate+5% magnesium sulfate solution, there was a significant increase of the mean chain length and Si/Al atom ratio in polymers of the 8FASS specimen, while other specimens did not experienced significant changes.

3.4. Scanning Electron Microscopy (SEM), fracture surfaces

Specimens taken from the surface were examined using SEM in the mode of secondary electrons. Fig. 12(A–C) shows the geopolymer specimens 8FA, 8FASS and 8FAK before the test. The specimens activated by sodium hydroxide (8FA) and by sodium hydroxide and potassium hydroxide (8FAK) solutions had more crystalline appearance than the specimens activated by sodium silicate (8FASS).

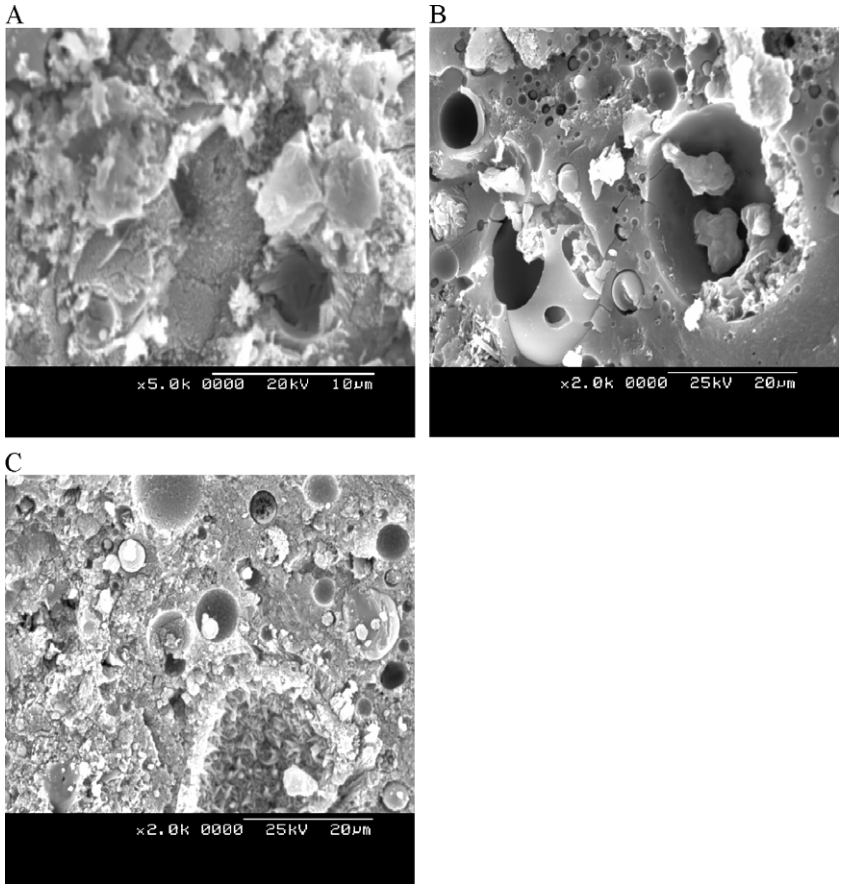

Fig. 13. SEI of geopolymer samples after 2 months exposure to 5% sodium sulfate solution: (A) 8FA, (B) 8FASS, (C) 8FAK.

For the analysis, the samples were taken from the surface (0–1 mm depth) exposed to the solutions. Fig. 13(A–C) shows the SEI of the 8FA, 8FASS and 8FAK materials exposed to the 5% sodium sulfate solution for 2 months. In all three specimens, some new gel-like phases appeared in the microstructure. As a result of that, quite dense microstructure developed particularly in the 8FA specimen. Fig. 14(A–C) presents the SEI of the 8FA, 8FASS and 8FAK materials exposed to 5% magnesium sulfate solution for 2 months. Lightly coloured precipitates can be seen in all three geopolymeric specimens. The effect of the test on the microstructure was more significant for the material formed with sodium hydroxide solution than for materials formed by activation with sodium silicate solution. The precipitates in the 8FA and 8FAK specimens were more significant than in the 8FASS specimen. In the 8FA and 8FAK specimens, exposure to the magnesium sulfate solution resulted in a dense microstructure in the surface region.

Fig. 15(A–C) shows the geopolymer specimens 8FA, 8FASS and 8FAK, respectively, exposed to 5% sodium sulfate+5% magnesium sulfate solution for 2 months. SEM observations indicated that specimens exposed to this solution had lightly coloured precipitate (Fig. 15(A–C)). The most significant precipitate was observed in the 8FAK specimen.

3.5. Backscattered electron imaging (BEI) and microanalysis

Although visual examination of the geopolymer specimens did not reveal any signs of deterioration after 5 months of immersion, microscopical examination of the 8FAK specimens showed vertical cracks extending from the surface to depths of 10–15 mm (Fig. 16(A–B)). Examination of the specimens in the SEM BEI showed presence of deep vertical cracks in the 8FAK specimens after exposure to different solutions; no such cracks were found in the 8FA and 8FASS specimens (Fig. 17(B)). The vertical cracks were spaced 10 to 15 mm apart. Fig. 16(A–B) shows typical cracking present in the 8FAK specimens. The specimens had insignificant difference in spacing of vertical cracks and their depth. The 8FAK specimens had deeper cracks when exposed to 5% solutions of sodium sulfate and magnesium sulfate, than that after exposure to the solution of 5% magnesium sulfate+5% sodium sulfate. Table 6 summarises the microscopical observations. In addition, formation of small amount of silica-rich precipitate, which also contained Mg was observed in the 8FAK specimens above deep vertical crack (Figs. 17(A) and 18).

The 8FASS, 8FA and 8FAK specimens exposed to magnesium sulfate solutions were studied using X-ray microanalysis. The bulk chemical variation of Ca, Si, Al,

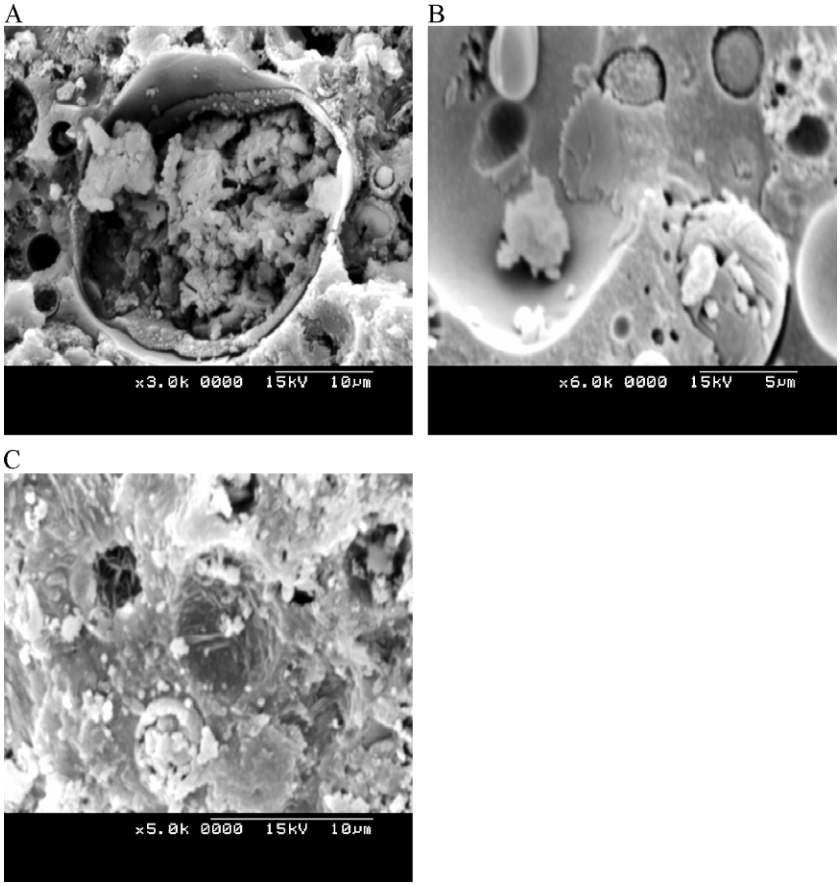

Fig. 14. SEI of geopolymer samples after 2 months exposure to 5% magnesium sulfate solution: (A) 8FA, (B) 8FASS, (C) 8FAK.

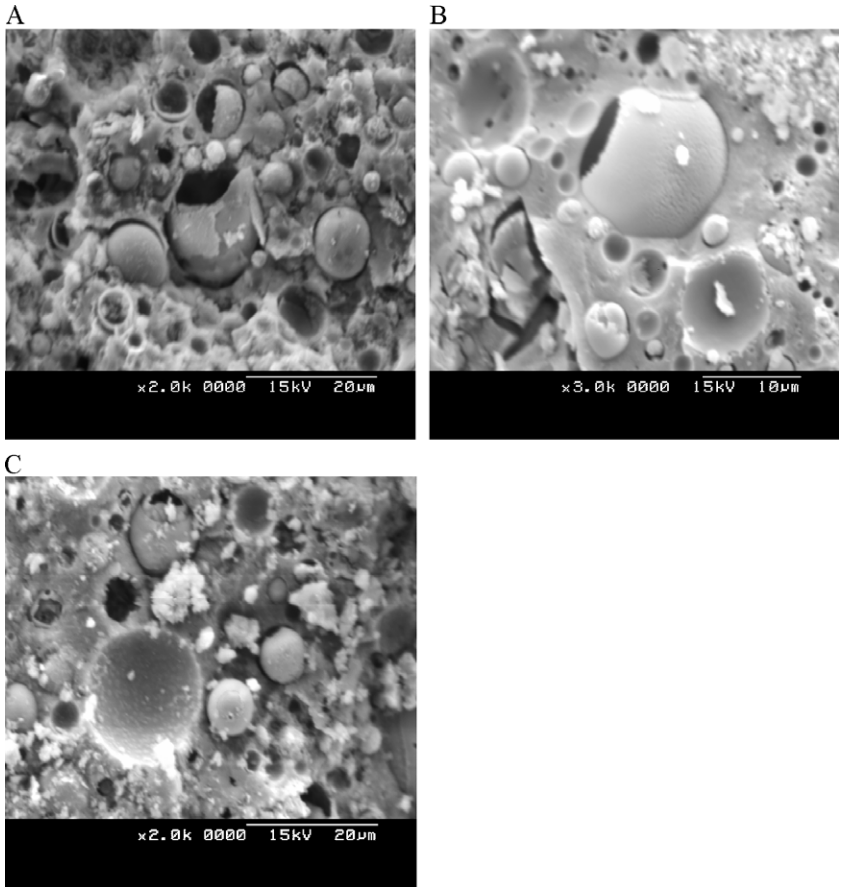

Fig. 15. SEI of geopolymer samples after 2 months exposure to 5% magnesium sulfate+5% sodium sulfate solution: (A) 8FA, (B) 8FASS, (C) 8FAK.

S and Mg as a function of depth is shown in Fig. 19 for the 8FAK specimen. The bulk chemical concentration was obtained by collecting X-rays from the fields laying at different depths from the surface, from 0 to 13000 μm. Each field had the same width of 200 mm and represented an area of 34,000 μm^2. Each field was rastered over its whole area. The emitted X-ray was collected for 200 s and processed employing the ZAF-correction procedure. An increase of Ca (5–10%) and Mg (about 5%) concentrations in the subsurface area was observed in the 8FASS and 8FAK specimens.

3.6. ICP-OES and ion chromatography

An additional analysis of the testing media was performed using ICP and ion chromatography. Table 7 presents the results of measurements of the pH of the solutions and the K^+, Na^+, SO_4^{-2}, Mg^{+2} ion concentrations in the media before and after the immersion of geopolymer specimens. In the sodium sulfate solution, the measurements showed an increase of Na^+ concentration 6–9% in the case of the 8FA and 8FASS specimen immersion, and

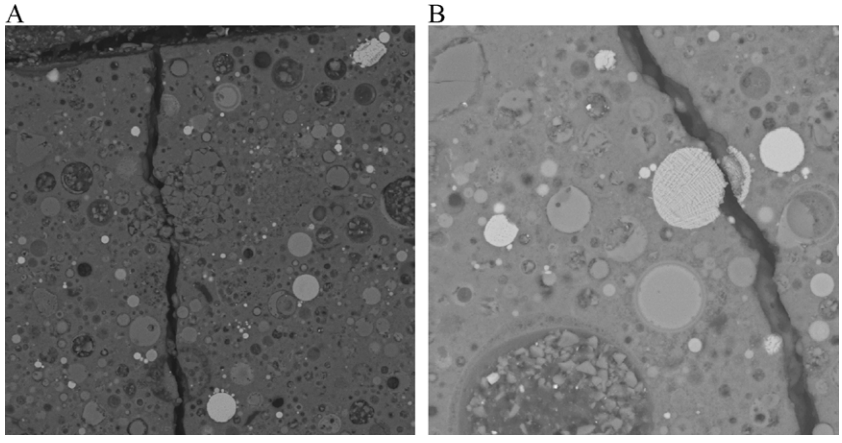

Fig. 16. BEI of geopolymer samples 8FAK after 5 months exposure to (A) 5% $MgSO_4$ solutions, (B) 5% Na_2SO_4 solution.

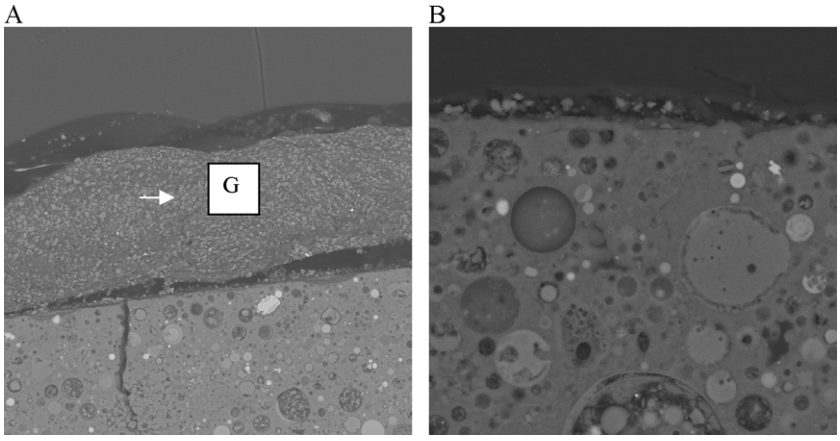

Fig. 17. BEI of geopolymer samples after 5 months exposure to 5% $MgSO_4$ solutions, surface area: (A) prepared using a mixture of sodium hydroxide and potassium hydroxide solutions (8FAK), (B) prepared using sodium hydroxide solution (8FA). G=precipitate formed above a deep vertical crack.

a considerable 33% increase in the case of the 8FAK specimens. In the magnesium sulfate solution, the analysis also indicated an increase of Na^+ concentration for immersion of all three specimens, and decline of $[Mg^{+2}]$ in testing solutions in the case of the 8FASS and 8FAK specimens. In the case of 5% sodium sulfate+5% magnesium sulfate solution, the analyses indicated a small increase of Na^+ concentration, and decline of $[Mg^{+2}]$ and $[SO_4^{-2}]$ in testing solutions in the case of immersion of all three specimens.

4. Discussion

It could be expected that interaction of geopolymer materials with sulphate solutions is significantly different from OPC because of the nature of aluminosilicate gel in geopolymeric materials. In fact, the results of the experiments showed that the tested geopolymer materials had very different durabilities when exposed to sulfate solutions. The most significant changes in the microstructure and compressive strength were induced by immersion in the 5% sodium sulfate and 5% magnesium sulfate solutions. Immersion in the solution of 5% sodium sulfate+5% magnesium sulfate had the least impact on strength of the materials. It appeared that immersion in more concentrated solution produced fewer changes in the strength of the geopolymers than immersion in less concentrated ones. This observation was opposite for OPC specimens, which had the most significant deterioration in concentrated solution, which is supported by weight and strength changes (Tables 3 and 4).

4.1. Sodium sulfate solution

In the solution of sodium sulfate, the strength of the 8FA specimens had 4% increase over the time of experiment. However, the strength of the 8FAK specimens declined rapidly, and in the 8FASS specimens, compressive strength fluctuated and had 18% reduction over 5 months of the experiment. The measurements of the pH of the solution and the K^+, Na^+, SO_4^{-2}, Mg^{+2} ion concentrations by ICP and ion chromatography before and after the immersion of geopolymer specimens indicated that the interaction with the testing solutions containing sodium sulfate caused migration of alkali ions from the specimens into the solution. The migration of alkalies was particularly high in the case of the 8FAK specimens in 5% sodium sulfate solution. There was a significant increase of pH of the media in which the 8FAK specimens were immersed, and very high strength loss was measured in the specimens. The mode of failure of the 8FAK samples after exposure to the sodium sulfate solution

Table 6
Summary of BEI observations

Specimen's ID, type of medium	Type of cracking	Spacing of vertical cracks (mm)	Depth of cracks from the surface (mm)
8FA, 5% Na_2SO_4 solution	No cracking	–	–
8FA, 5% $MgSO_4$ solution	No cracking	–	–
8FA, 5% Na_2SO_4+5% MgSO4 solution	No cracking	–	–
8FASS, 5% Na_2SO_4 solution	No cracking	–	–
8FASS, 5% $MgSO_4$ solution	No cracking	–	–
8FASS, 5% Na_2SO_4+5% $MgSO_4$ solution	No cracking	–	–
8FAK, 5% Na_2SO_4 solution	Vertical cracks	10–15	10–15
8FAK, 5% $MgSO_4$ solution	Vertical cracks	10–15	5–15
8FAK, 5% Na_2SO_4+5% $MgSO_4$ solution	Vertical cracks	10–15	1–5

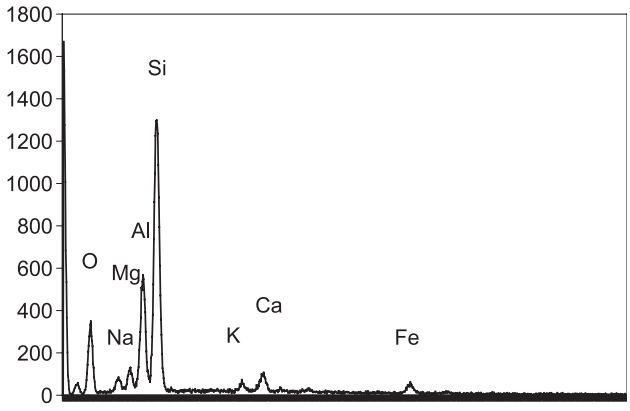

Fig. 18. EDS spectrum of the precipitate G (at arrow in Fig. 17(A)) in 8FAK specimen after 5 months exposure to 5% $MgSO_4$ solution.

indicated that some microcracks may have formed during immersion. SEM study of the polished specimens confirmed the presence of deep vertical microcracks in the 8FAK specimens, which extended 10–15 mm from the surface. Apparently, there was a significant loss of strength in these specimens as a result of microcrack development. Possibly, these microcracks formed as a result of stresses caused by diffusion of K^+ and Na^+ ions outside the geopolymer specimens into the sodium sulfate solution. No such cracks were observed in the material 8FA prepared using sodium hydroxide. Although no deep cracks were observed in the 8FASS specimen, it is possible that they may develop in this material with time, because up to 20% deterioration of strength was measured in these specimens. In addition, formation of ettringite may contribute to the deterioration of the 8FASS specimens in sulfate solutions.

The fly ash materials formed by geopolymerisation can best be viewed as a matrix of amorphous alkali aluminosilicate gel with residue of fly ash imbedded in it [7–9]. Davidovits proposed that aluminosilicate gel in geopolymers consists of a polymeric Si–O–Al framework, with SiO_4 and AlO_4 tetrahedra joint by sharing O atoms [10,11]. Al is tetrahedrally coordinated in this network and has a net negative charge. Thus, to maintain electroneutrality, the presence of cations, such as Na^+, K^+ and Ca^{2+}, is essential for charge balance of tetrahedrally coordinated Al. In zeolites and aluminosilicate gels, Na^+ and K^+ can be exchanged if the material is placed in solutions of salts containing replacing cations [14,15]. The exchange rate depends on the permeability of the material, which is controlled by the average pore diameter. The 8FAK specimens had the highest exchange rate due to largest pore diameter [16,17], and the 8FAK specimens had the highest strength loss; next in the pore size was the 8FASS material, which had the next, after 8FAK, strength loss in the immersion experiments. The migration of Na^+ into the solution must be connected to development of vertical cracks, which are responsible for deterioration of strength in materials prepared using a mixture of sodium hydroxide and potassium hydroxide. Therefore, in the sodium sulfate solution, migration of alkali cations into the contact solution is the most significant cause of strength loss in some of geopolymer materials.

4.2. Magnesium sulfate solution

In the solution of magnesium sulfate, compressive strength of tested geopolymer specimens fluctuated, but only in the case of the 8FASS specimens where it had a 24% reduction, while in the 8FA and 8FAK specimens, after 6 months, compressive strength increased 12% and 35%, respectively. SEM examination revealed formation of deep vertical cracks in the 8FAK specimens exposed to magnesium sulfate solutions. ICP and ion chromatography indicated migration of alkali cations into solution. The analysis also indicated a decline of $[Mg^{+2}]$ in testing solution in the case of the 8FASS and 8FAK specimens, which may occur due to migration of Mg^{2+} into material. Bulk chemical variation across the specimens showed an increase of Ca, Mg and S concentrations in the surface

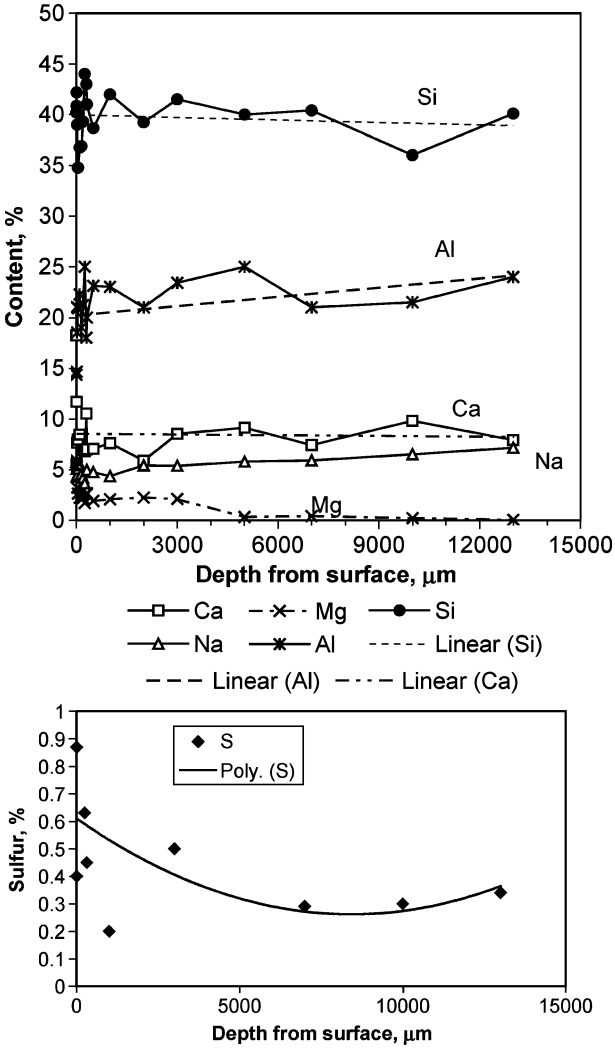

Fig. 19. Chemical variation in the 8FAK specimen as a function of distance from surface. 8FAK sample was analysed after exposure to 5% $MgSO_4$ solution.

Table 7
Chemical analysis of solutions after immersion of geopolymer specimens by ICP-OES and ion chromatography

Sample ID, type of media	pH	$[Na^+]$	$[K^+]$	$[Mg^{+2}]$	$[SO_4^{-2}]$
8FA in 5% Na_2SO_4	8.58	0.67	0.00	0.00	0.335
8FASS in 5% Na_2SO_4	9.14	0.65	0.00	0.00	0.325
8FAK in 5% Na_2SO_4	11.64	0.81	0.01	0.00	0.41
8FA in 5% $MgSO_4$	8.22	0.06	0.00	0.21	0.21
8FASS in 5% $MgSO_4$	7.91	0.05	0.00	0.20	0.23
8FAK in 5% $MgSO_4$	9.51	0.08	0.01	0.19	0.22
8FA in 5% $MgSO_4$+5% Na_2SO_4	8.67	0.73	0.00	0.22	0.52
8FASS in 5% $MgSO_4$+5% Na_2SO_4	8.43	0.75	0.00	0.16	0.54
8FAK in 5% $MgSO_4$+5% Na_2SO_4	8.73	0.73	0.02	0.16	0.54
Initial solution 5% Na_2SO_4	7.79	0.61	0.00	0.00	0.34
Initial solution 5% $MgSO_4$	7.05	0.00	0.00	0.21	0.21
Initial solution 5% $MgSO_4$+5% Na_2SO_4	7.40	0.72	0.00	0.24	0.55

Ion concentration in mol/l.

area, a slight decrease of Al content, while Si content stayed without change. Therefore, migration of Ca from inside of the specimen to the surface area, and S and Mg from the solution into aluminosilicate matrix can be suggested [8]. The SEM examination of fracture surface (Fig. 14(A–C)) has shown formation of lightly coloured precipitates in the surface area of the 8FASS, 8FAK and 8FA samples exposed to magnesium sulfate solution. In these solutions, the diffusion of Mg into material occurred at the same time as migration of alkali ions from samples into solution. These processes are possibly responsible for fluctuations of the compressive strength and final strength improvement of the 8FA and 8FAK specimens when immersed in the magnesium sulfate solution. Ca^{+2} and Mg^{+2} ions can be accommodated in aluminasilicate gel as network-modifying cations [18]. The migration of these ions into aluminosilicate gel seemed to improve the strength of the 8FA and 8FAK geopolymer specimens regardless of the development of deep vertical cracks in the 8FAK due to migration of Na from the specimens into the solution. However, in the solution of magnesium sulfate, the 8FASS specimens had a significant reduction of strength, which was possibly caused by migration of alkalies into the solution and formation of ettringite in the surface area as was suggested by XRD analysis (Fig. 7). Therefore, different reaction products were formed in the 8FASS, 8FA and 8FAK specimens as a result of interaction with magnesium sulfate solution.

Different durabilities of the tested specimens when exposed to sulfate solutions must be connected to the different aluminosilicate gel structures. The 8FA specimens were the most stable in the sodium sulfate and magnesium sulfate solutions, as compared to the 8FASS and 8FAK specimens. Previous investigation indicated that the aluminosilicate gels in the studied materials possess different degrees of ordering, and in the 8FA specimen, it was more crystalline than that in the 8FAK and 8FASS specimens [11,17]. Previous investigations also indicated that the 8FA specimens were more resistant to acid attack as compared to the 8FASS and 8FAK specimens, which had very significant loss of strength in sulfuric acid solution [16]. Thus, good durability of the 8FA specimens prepared using sodium hydroxide in sulfate and acid environments was attributed to more stable cross-linked polymer structure as compared to the 8FASS and 8FAK specimens prepared using sodium silicate and a mixture of sodium and potassium hydroxides, respectively.

The stability of strength of the tested geopolymeric specimens depended on the type of activator used in specimen preparation. The specimens prepared with sodium hydroxide were more durable than specimens prepared with sodium silicate activator and a mix of sodium and potassium hydroxides. The durability is possibly dependent on the average pore size of the tested specimens. The results of BET analysis indicated that the average pore diameter in 8FA sample was 45 Å, while in the 8FASS and 8FAK samples, it was 63 and 116 Å, respectively, while the BET surface area was 43 m^2/g in the 8FA, and about 14 m^2/g in the 8FASS and 8FAK specimens [16,17]. Therefore, good durability of the 8FA specimens was possibly linked to their nanoporous structure with very fine pores. Although both materials, the 8FAK and 8FA, contained traces of poorly crystalline zeolites, the 8FAK samples had significantly larger average pore size measured by gas adsorption and thus were more permeable by the sulfate solutions.

The stability of the tested geopolymeric specimens depended on the type of cation in the sulfate media. Immersion into the sodium sulfate solution caused migration of the alkalies from geopolymer materials into the solution and resulted in significant fluctuations of strength in the specimens with loosely bound alkalies. In the magnesium sulfate solution, there was a precipitation of gel containing Mg and Ca ions particularly in the pores of the specimens 8FAK and 8FA prepared with sodium hydroxide activator. SEM examination indicated a reduction in porosity of the surface layer, which can be linked to strength improvement in the 8FAK and 8FA specimens, while in the 8FASS, precipitation of ettringite possibly contributed to strength deterioration.

In the solution of magnesium+sodium sulfate, there were both migration of alkalies into the solution and precipitation of gel in the microstructure, which resulted in less impact on the strength of materials than in the other two cases. In addition, because of higher ionic strength of the testing solution, less diffusion of alkalies into the solution was observed in the case of magnesium+sodium sulfate solution (Table 7). Observation of microcrack pattern in the geopolymer materials exposed to sulfate environment led to suggestion that durability of these materials could be greatly improved by introduction of aggregates.

Most laboratory methods aimed at studying the sulfate attack mechanism are based on accelerated methods [7,8,19]. The tests in this investigation utilised two accelerating methods: increasing reaction surface (small specimens/large surface areas) and increasing concentration of solutions. In most practical situations, sulfate solution concentration in the ground water and soil are low (<1000 ppm SO_3). It is considered impractical to use such low-level concentrations; thus, accelerating sulfate attack is a necessity [19]. The investigation utilised two levels of concentrations: 5% Na_2SO_4, 5% $MgSO_4$, and 5% Na_2SO_4+5% $MgSO_4$, to investigate the effect of such high concentration levels on the mechanism of sulfate attack. An increased concentration of 5% Na_2SO_4+5% $MgSO_4$ solution was utilised to see if this will induce a different deterioration mechanism in the geopolymeric materials. It was found that in the more concentrated solution, which utilised both 5% Na_2SO_4 and 5% $MgSO_4$, the deterioration of strength was less than in 5% Na_2SO_4 and 5% $MgSO_4$ solutions. This investigation did not utilise sulfate solution concentration found in the ground water and soil, but it is recommended for future study, because the deterioration mechanism is diffusion related, in which case maximum gradient of concentration may present the most significant deterioration.

5. Conclusions

The geopolymer specimens had very different durabilities when exposed to sulfate solutions. The stability of the tested geopolymeric specimens depended on the type of activator used in specimen preparation and concentration and type of cation in the sulfate media. The least changes in geopolymer specimens were found in the solution of 5% sodium sulfate+5% magnesium sulfate. The most significant fluctuation of strength and microstructural changes took place in 5% solutions of sodium sulfate and magnesium sulfate. In the solution of sodium sulfate, migration of alkalies from geopolymer specimens into the solution was observed. Diffusion of alkali ions into the solution caused significant stresses and formation of deep vertical cracks in the specimens prepared using a mixture of sodium and potassium hydroxides. In magnesium sulfate solution, in addition to migration of alkalies from geopolymers into the solution, there was also diffusion of Mg and Ca in the surface layer of geopolymers, which improved their strength. In material prepared using sodium silicate, formation of ettringite was also observed, which contributed to a loss of strength.

The best performance in different sulfate solutions was observed in the geopolymer material prepared with sodium hydroxide and cured at elevated temperature. These specimens had 4–12% increase of strength when immersed into sulfate solutions. Good performance was attributed to a more stable cross-linked aluminosilicate polymer structure. Specimens prepared with sodium hydroxide were more stable in sulfate solutions than specimens prepared using sodium silicate or mixture of sodium and potassium hydroxide solutions.

Acknowledgements

The author is grateful to the Australian Research Council for financial support under Grant DP0209501 and Civil Engineering Department and School of Physics and Materials Engineering, Monash University, for providing access to equipment used in this investigation. The author would like to thank Dr. M. Cohen for his helpful comments and encouragement.

References

[1] P.K. Mehta, Sulfate attack on concrete: a critical review, in: R.R. Villarreal (Ed.), Concrete Durability, Univ. Autonoma de Nuevo Leon, 1993, pp. 107–132.
[2] L.D. Wakely, T.S. Poole, J.J. Ernzen, B.D. Neeley, Salt saturated mass concrete under chemical attack, in: P. Zia (Ed.), High Performance Concrete in Severe Environments, Am. Concr. Inst., vol. SP-140, 1993, pp. 239–267.
[3] E.F. Irassar, A. Di Maio, O.R. Batic, Sulfate attack on concrete with mineral admixtures, Cem. Concr. Res. 26 (1) (1996) 113–123.
[4] C.F. Ferraris, J.R. Clifton, P.E. Stutzman, E.J. Garbocsi, Mechanisms of degradation of Portland cement-based systems by sulfate attack, in: K.L. Scrivener, J.F. Young (Eds.), Mechanisms of Chemical Degradation of Cement-Based Systems, E and FN Spon, London, 1997, pp. 185–192.
[5] M. Santhanam, M.D. Cohen, J. Olek, Mechanism of sulfate attack: a fresh look: Part 2. Proposed mechanisms, C&CR 33 (2003) 341–346.
[6] H.F.W. Taylor, R.S. Gollop, Some chemical and microstructural aspects of concrete durability, in: K.L. Scrivener, J.F. Young (Eds.), Mechanisms of Chemical Degradation of Cement-Based Systems, E and FN Spon, London, 1997, pp. 177–184.
[7] D. Bonen, M. Cohen, Magnesium sulfate attack on Portland cement paste: I. Microstructural analysis, Cem. Concr. Res. 22 (1992) 169–180.
[8] D. Bonen, M. Cohen, Magnesium sulfate attack on Portland cement paste: II. Chemical and mineralogical analyses, Cem. Concr. Res. 22 (1992) 707–718.
[9] A. Palomo, M.W. Grutzeck, M.T. Blanco, Alkali-activated fly ashes a cement for the future, Cem. Concr. Res. 29 (1999) 1323–1329.
[10] J.C. Swanepoel, C.A. Strydom, Utilisation of fly ash in a geopolymeric material, Appl. Geochem. 17 (2002) 1143–1148.
[11] T. Bakharev, Geopolymeric materials prepared using class F fly ash and elevated temperature curing. Accepted for publication in C and CR, 2004.

[12] D. Hardjito, S.E. Wallah, B.V. Rangan, The engineering properties of geopolymer concrete, Proceedings of the Int. Conf. Geopolymer, 28–29 October 2002, Melbourne, Australia 2002.
[13] J.G.S. van Jaarsveld, J.S.J. van Deventer, The effect of metal contaminants on the formation and properties of waste-based geopolymers, Cem. Concr. Res. 29 (1999) 1189–1200.
[14] H. Van Bekkum, E.M. Flanigen, J.C. Jansen, Introduction to Zeolite Science and Practice, Elsevier, Amsterdam, 1991.
[15] D.W. Breck, Zeolite Molecular Sieves: Structure, Chemistry and Use, Wiley-Interscience, New York, 1974, p. 338, 415–418.
[16] T. Bakharev, Resistance of Geopolymer materials to acid attack. Accepted for publication in C and CR, 2004.
[17] T. Bakharev, Porosity and microstructure of geopolymer materials utilising class F fly ash, submitted for publication in C and CR, 2004.
[18] D.C. Perera, M.G. Blackford, E.R. Vance, J.V. Hanna, K.S. Finnie, C.L. Nicholson, Geopolymers for the immobilization of radioactive waste, presented at MRS Spring Meeting April 11–15, 2004, San Francisco, to be published.
[19] M.B. Cohen, B. Mother, Sulfate attack on concrete-research needs, ACI Mater. J. 88 (1) (1991) 62–69.